

Seismic Performance Comparison of Moderately Ductile and Conventional Construction Steel Concentrically Braced Frames



Anirban Kundu, Lydell Wiebe, and Georgios P. Balomenos

Abstract Steel concentrically braced frames (CBFs) are widely used as a seismic force resisting system (SFRS) in Canada because of their efficiency in resisting seismic loads. Several different approaches can be taken to design CBFs according to the Canadian Steel Design Standard CSA S16:19. These approaches range from moderately ductile (Type MD) CBFs, which require special detailing considerations and limits on local and member slenderness to promote the intended ductile response, to conventional construction (Type CC), which requires higher seismic design forces but has more relaxed detailing requirements. While these construction types have been defined in CSA S16:19 for many years, few studies have compared the seismic performance of frames designed using these different sets of requirements. To address this research gap, this paper compares designs for the same archetype structure using both Type MD and Type CC CBFs. Both frame types are designed according to CSA S16:19 and subsequently modelled using the advanced earthquake simulation software OpenSees. Thereafter, the models are subjected to a multiple stripe analysis (MSA) using a set of ground motions prescribed in FEMA P-695, to assess their seismic performance. A close look at the inter-storey drift time history during a typical ground motion record reveals the sequential occurrence of the different damage states, while the statistics of the inter-storey drift ratio demonstrates that the Type CC design leads to more variable performance. Finally, storey-by-storey fragility curves are developed for both construction types to compare the seismic performance.

Keywords Seismic performance · Steel structures · Numerical modelling · Concentrically braced frames · Conventional construction · Moderately ductile concentrically braced frame · Multiple stripe analysis

A. Kundu (✉) · L. Wiebe · G. P. Balomenos
Department of Civil Engineering, McMaster University, Hamilton, Canada
e-mail: kundua6@mcmaster.ca

© Canadian Society for Civil Engineering 2023
R. Gupta et al. (eds.), *Proceedings of the Canadian Society of Civil Engineering Annual Conference 2022*, Lecture Notes in Civil Engineering 348,
https://doi.org/10.1007/978-3-031-34159-5_18

1 Introduction

Concentrically braced frames (CBFs) are widely used as a lateral force resisting system for their inherent strength and stiffness, which make them efficient, economical, and practical to meet the force and deformation requirements of building codes. The lateral force is resisted by the tension and compression of opposing braces. During severe, infrequent earthquakes, braces yield in tension and buckle in compression, and the post-buckling behaviour of the brace is associated with formation of a hinge at mid-length, as well as significant cyclic load and end rotational demand on the gusset plate [11]. To promote the intended brace behaviour, modern seismic codes place limits on the global and local slenderness ratios of brace sections for the most ductile CBFs (e.g., Type MD CBFs in [7]). Meanwhile, other framing elements are required to be capacity protected to remain elastic when the braces reach their probable post-buckling and post-yielding strengths. Also, the connections of the braces to the framing elements must be designed and detailed properly so that the ductile failure mechanism is concentrated only in the brace. The most critical detailing parameters include adequate rotational capacity in the gusset plate at the brace ends, as well as adequate weld strength and toughness (hereafter referred to as a “demand critical weld”) at the gusset plate interface and brace-to-gusset connection. A recent extension of this approach is the balanced design procedure (BDP), where a preferred sequence is promoted for the different yielding and failure mechanisms in an effort to maximize the overall ductility [22].

When such design requirements are not followed, the consequences can include loss of strength and stiffness of the brace module at low drift demands, leading to a premature and unintended system failure mechanism. Such behaviour is expected for CBFs built prior to modern seismic ductility design provisions, referred to as non-ductile CBFs (NCBFs) [25]. Alternatively, modern seismic codes generally allow lower ductility CBFs to be designed for higher seismic forces as a means to avoid the above-mentioned complexities of ductile designing while also avoiding unintended failure modes. For example, the US standard (ASCE/SEI 7-22 2022) has categories for “*system not specifically detailed for seismic resistance*” ($R = 3$) and ordinary CBF (OCBF, $R = 3.25$), while the Canadian standard [7] has categories for limited ductility (LD) CBFs and conventional construction (CC). While a relatively high ductility-related reduction factor ($R_d = 3.0$) allows Type MD CBFs to be designed with a relatively low base shear, Type CC CBFs are designed with a comparatively lower value of R_d (1.5), leading to a higher base shear but without the need for rigorous seismic detailing. CSA S16:19 prescribes a further 50% increase in the connection demand for Type CC design when the expected connection failure mode is not ductile. Although there are some limitations to the use of Type CC, such as excluding it for post-disaster buildings [20] there are few limitations on designing or detailing. This ease of design makes it convenient for a designer to use Type CC design as a seismic force resisting system (SFERS), particularly in regions of low or moderate seismicity. On the other hand, these relaxations may make the seismic performance of Type CC design less predictable. The behaviour might be expected

to be similar to the NCBFs due to the following reasons: (i) CSA S16:19 implies a preference for ductile connections but does not define how to do this; (ii) lack of adequate rotational clearance at the brace ends could cause fracture of the interface welds, leading to the complete loss of connection strength and hence the total brace module [24], and (iii) absence of limitations for local and global slenderness ratio in the braces, which might lead to premature fracture of them. The difference between Type MD and Type CC CBFs in both seismic design loads and expected nonlinear response leads to uncertainty about their relative performance overall.

The seismic performance of Type CC CBFs was studied by [6] in two phases. First, the ductility capacity of a typical bolted brace connection was evaluated experimentally. Based on the force and deformation ductility capacity found in first phase, a set of buildings was designed and analysed numerically with varying design parameters such as location (Vancouver and Montreal), building height, storey height, bracing configuration, etc. Among the set, two buildings from Vancouver were chosen for incremental dynamic analysis. The study suggested that connections need to be designed with demand related to $R_d R_o$ less than 1 to avoid any height limit, but buildings with a height of 15.6 m or less would provide adequate protection against collapse if ductile connections are used, the building is located on Site Class C, and a split-X or chevron configuration is used. In the USA, experimental testing of one-storey, single-diagonal-configuration bracing systems was performed at the University of Washington to investigate the behaviour of Special CBFs (SCBFs), which are the most ductile CBF system according to the AISC Seismic Provisions (ANSI/AISC 341-16 2016), as well as NCBFs, under a quasi-static loading protocol. The behaviour of SCBFs was experimentally demonstrated by [10, 15, 16, 21]. Subsequently, the same frame configuration was used by [4, 14, 27, 28] to investigate the behaviour of the CBFs designed non-seismically, along with various types of connection and their behaviour after retrofit. Based on the results from these experimental tests, an improved numerical approach was developed to model the gusset plate connection for both SCBFs (which are similar to Type MD CBFs, as per CSA S16:19) [12], as well as NCBFs [24].

A few other studies are also important in the context of seismic behaviour of non (or low)-ductile CBFs. [23] tested six full-scale Type CC I-shaped brace specimens with bolted end connections in two different configurations to connect the brace to the gusset plate. The test indicated that the Type CC brace specimens could achieve storey drift ratios of 1–2%, even though capacity design provisions were not incorporated in their design. Significant contributions to ductility capacity came from yielding and buckling of the gusset plate and lap plate, together with bolt bearing, and friction associated with bolt slip. Based on the findings of [23], a component-based numerical modelling approach was proposed by [29], which takes into account the considerable contribution of gusset plate yielding and bolt hole elongation to overall deformation capacity. Two full-scale, two-storey, low-ductility CBFs, one with seismic detailing as per the AISC Seismic Provisions (ANSI/AISC 341-16 2016) for an ordinary concentrically braced frame (OCBF) with $R = 3.25$ and another with no seismic detailing ($R = 3$), were tested by [5]. The study evaluated failure mechanisms, post-elastic frame behaviour, reserve capacity, and overall

collapse performance. A detailed seismic performance assessment of low-ductility CBFs, in the context of US design standard, was conducted by [26].

Building on these past studies of the performance of CBFs, this study develops a storey-wise collapse-based fragility assessment considering three damage states. First, a pair of 3-storey CBFs are designed according to Clauses 27.5 (Type MD, $R_d = 3$, $R_o = 1.3$) and 27.12 (Type CC, $R_d = 1.5$, $R_o = 1.3$) of [7], using seismic force demands calculated as per the National Building Code [20]. Next, numerical models are developed to capture fracture in the brace for both Type CC and MD CBF, as well as fracture of the gusset plate interface weld in the case of Type CC CBF. A suite of 44 ground motions is then chosen based on the [9] and scaled based to the design spectrum. The seismic performance is investigated first for a single ground motion at design ground motion (DGM) level earthquake. Next, a series of nonlinear response history analyses (NLRHA) are conducted in OpenSees [19] under the framework of multiple stripe analysis [3]. Finally, the fragility curves obtained from both the design types are compared.

2 Specimen Design

Figure 1 shows the three-storey office building that was considered in this study, located in Victoria, BC, and having a total height of 12.5 m, with a plan dimension of 36 m \times 36 m and bay lengths of 9 m in each direction. The gravity loads are shown in Table 1. The prototype building was equipped with two braced bays in each exterior frame. The brace configuration was split-X cross bracing at the first two storeys and chevron at the top storey. Site Class C was considered with an importance factor of 1. The design spectrum was calculated based on the hazard level for a 2% probability of exceedance in 50 years, noted as the design ground motion (DGM) as per the [20]. The R_d for Type MD design is 3, whereas for Type CC it is 1.5. For the Type MD design, the base shear was 7075 kN, whereas it was 14,150 kN for Type CC design. The modelled fundamental period of the Type MD CBF was 0.35 s, whereas for the Type CC CBF, it was 0.33 s. The designed member dimensions are provided in Table 2.

As $I_E S_a(0.2) > 0.45$, the connection demand was amplified by 50% of the factored brace force demand [7]. To differentiate from the Type MD design, capacity-based designing details were not followed in the Type CC design, including:

- In the case of Type MD design, the beams were designed for the factored gravity load along with an unbalanced vertical force demand generated due to the difference between the expected post-buckling capacity of the compression braces and the expected yielding capacity of the tension braces. This unbalanced demand was also considered in designing the shear tab connections at the beam ends. In Type CC design, this unbalanced vertical force demand was not considered when designing the beam. Likewise, the shear tab connection at the end of the beam was designed for the factored gravity load only.

Fig. 1 Floor plan and the elevation of the building

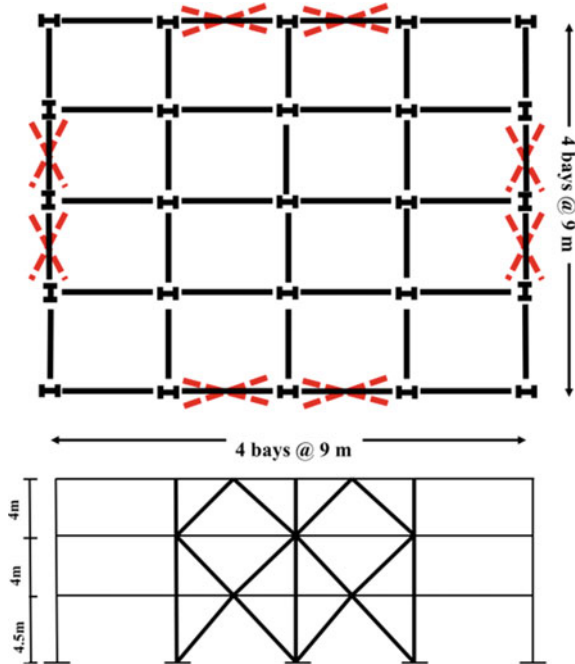


Table 1 Gravity loads

| | Load (kPa) | | | |
|-------|------------|------|------|----------|
| | Dead | Live | Snow | Cladding |
| Roof | 3.5 | 1.0 | 1.64 | 1.5 |
| Floor | 4.9 | 2.4 | – | |

Table 2 List of designed members

| St | Type MD | | | Type CC | | |
|----|------------|------------|-------------------|-----------|------------|--------------------|
| | Beam | Column | Brace | Beam | Column | Brace |
| 3 | W610 × 341 | W310 × 415 | HSS127 × 127 × 13 | W410 × 46 | W360 × 134 | HSS203 × 203 × 7.9 |
| 2 | W460 × 97 | | HSS152 × 152 × 13 | W460 × 60 | | HSS254 × 254 × 9.5 |
| 1 | W610 × 415 | | HSS178 × 178 × 16 | W460 × 60 | | HSS254 × 254 × 16 |

- The global slenderness ratio of the braces in Type MD CBF was limited to a minimum of 70, which was not required in Type CC CBF design.
- For Type MD CBFs, the width-to-thickness ratio of the HSS cross section was limited to $330/\sqrt{F_y}$ (for $KL/r \leq 100$, , which was the case for each brace in this current study). This restriction in local slenderness was not required for Type CC design.
- When calculating the demand on the column in Type MD CBF, the probable tensile and compressive capacity of the braces were considered, as per capacity design principles. Also, an additional moment of $0.2ZF_y$ (as mentioned in clause 27.5.5.3 (b) of [7]) was applied. Conversely, in the case of Type CC CBF, the vertical component of the factored force induced by the braces was considered based on the linear elastic analysis under the applied seismic loads, and no additional moment was considered.
- For Type MD CBF, the demand in the connection was calculated based on the probable strength of the brace. For Type CC, this demand was calculated as 1.5 times the factored brace design force.
- None of the clearance criteria (neither linear 2tp nor elliptical 8tp) was fulfilled for the Type CC design.

Although the Type MD CBF was designed for half the base shear of Type CC CBF, other restrictions resulted in a much larger beam section (Table 2), especially in the first and third floors, to accommodate the unbalanced vertical demand mentioned above. The column section within the SFRS was also larger for the Type MD design compared to Type CC. The braces in Type MD design are stockier, having a higher global slenderness but lower local slenderness ratio compared to Type CC.

3 Numerical Modelling

To capture the overall seismic behaviour of the CBF system, it is important to accurately model several key features, including yielding in tension, buckling and post-buckling of the brace in compression, rotational deformations and yielding of the gusset plates, and local yielding of the beams and columns adjacent to the gusset plates. Although a well-designed Type MD CBF seldom reaches fracture of the braces or gusset plate, for Type CC, these are paramount modelling requirements. A schematic of the frame modelled in OpenSees [19] is shown in Fig. 2, where fibre-discretized distributed-plasticity-based beam–column elements were used for the defining the braces, beams, and columns, while concentrated-plasticity springs were used to define the gusset plate connections.

Sixteen nonlinear displacement-based beam–column elements were used along the length of the brace with an initial camber of 1/500 of the total length, in a sinusoidal shape, to initiate the buckling behaviour of the brace. Four integration points were considered for each element. The cross section of the HSS brace was discretized using four fibres across the thickness and depth in each direction, following the

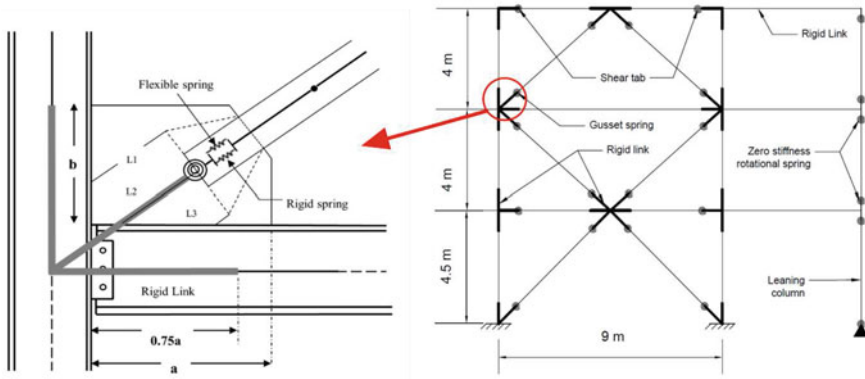


Fig. 2 Schematic diagram and numerical modelling details of the connection

approach recommended by [12]. Force-based nonlinear beam–column elements with four integration points were used for beams and columns along with fibre cross sections. To improve convergence during dynamic analysis in OpenSees, the beams were modelled with multiple elements, but without any imperfection, unlike the braces. A Giuffrè–Menegotto–Pinto model with the Steel02 material was used to model all the constitutive elements for all members [12, 24].

The gusset plate connection was simulated by using a zero-length nonlinear, concentrated, out of plane, rotational spring Hsiao et al. 2012), at the end of the brace in the axial direction where the rigid link ends (Fig. 2). Steel02 material was used as a constitutive model for the spring. The flexural stiffness (K) and strength (F_y^{rot}) of the rotational spring are provided in Eqs. (1) and (2) respectively, as follows:

$$K = \frac{E}{L_{avg}} \left(\frac{W_w t^3}{12} \right) \tag{1}$$

$$F_y^{rot} = \frac{W_w t^2 F_{y,gusset}}{6} \tag{2}$$

where E is Young’s modulus of steel, W_w is the Whitmore width defined by a 45° projection angle, L_{avg} is the average of $L1$, $L2$ and $L3$ as shown in Fig. 2, and t is the thickness of the gusset plate. The post-yield stiffness was taken as 1% of the initial stiffness. The rigid zones extend from the work point to the edge of gusset plate, except along the horizontal beam, where they extend to 75% of the gusset dimension. The shear tab (shown in Fig. 2) was modelled as per [18], as described by [8].

3.1 Fracture Modelling

The maximum strain-based fracture model developed by [13] and modified by [24] was used, where a fracture-material “wrapper” is used over the parent material. The fracture-material monitors the strain of the underlying parent material and initiates fracture of individual brace fibres based on the maximum strain range (MSR) between tension and compression. When the fracture criterion is reached, the strength and stiffness of the fibre are reduced by the wrapper to nearly zero. Conceptually, the fibre is removed from the section at that location, and the progressive fracture of the fibres leads to complete brace fracture. The MSR is a function of local as well as global slenderness ratio and strength of the material and is given by the following equation from [24]:

$$\text{MSR} = 0.554 \left(\frac{b}{t} \right)^{-0.75} \left(\frac{L_c}{r} \right)^{-0.47} \left(\frac{E}{F_y} \right)^{0.21} \left(\frac{\delta_{c,\max}}{\delta_{r,\max}} \right)^{0.068} \quad (3)$$

The above equation indicates that braces with a higher $\frac{b}{t}$ ratio lead to lower MSR, resulting in reduced fracture life. Ductile CBFs (e.g., Type MD in CSA S16:19) delay this behaviour by employing stockier cross sections. This factor creates a substantial difference in the fracture life in between braces in Type MD and Type CC design.

Another prevalent mode of failure in Type CC design is the gusset plate interface weld fracture, which leads to complete loss of strength provided by the brace module. This part of the connection is subjected to in-plane deformation due to the opening and closing of the beam–column joints, as well as out-of-plane deformation due to buckling of the brace. This is accommodated in ductile CBFs (Type MD in CSA S16:19 or SCBFs in AISC 341-16) by providing a clearance for brace end rotation along with demand critical welds. Conversely, in Type CC CBF, the connection was designed for an amplified force demand instead of applying this special ductile detailing. Shortcomings in the connection details of Type CC CBF in the modern code CSA S16:19 are like that of the NCBFs. So, the interface weld fracture was modelled with a rotational limit, θ_f (Eq. 4), proposed by [24]. The limit was employed on a zero-length rotational spring (shown in Fig. 2) defined for the gusset plate, proposed by [12]. The limit is a function of demand to capacity ratio for the interface weld (DCR_{gpw}) and the clearance provided at the end of the brace:

$$\theta_f = 0.11 \left(\frac{L_{\text{clear}}}{t_p} \right)^{0.33} \text{DCR}_{\text{gpw}}^{-0.57} \leq 0.257 \text{ rad} \quad (4)$$

where L_{clear} is the thickness of the elliptical clearance provided, and t_p is the thickness of the gusset plate. DCR_{gpw} was calculated according to the balanced design approach, proposed by [22], which was based on the tensile capacity of the plate and the weld, given by the following equation:

$$\text{DCR}_{\text{gpw}} = \frac{(R_y F_y)_p t_p}{0.9\sqrt{2}F_{EXX}w_p} \quad (5)$$

Type CC design was not expected to meet any of the criteria for clearance or demand critical welds. In most cases, the elliptical clearance factor ($\frac{L_{\text{clear}}}{t_p}$ in Eq. 3) was much lower than the prescribed value (i.e., 8, as per [7, 17]), near 1 or 2 or even less than that [25]. Therefore, to maintain uniformity and ease in modelling, $\frac{L_{\text{clear}}}{t_p}$ was taken as 1 when defining the model for all the gusset plates of Type CC, and in most of the cases the DCR was more than 1. The rotational spring was connected to the brace by a set of two parallel springs, one rigid and another one flexible. Once the amount of rotation in the gusset plate spring exceeds θ_f , the rigid spring (Fig. 2) was removed, causing all the axial resistance of the brace to be lost.

3.2 Model Validation

The numerical modelling approach was validated based on two experimental programs conducted at the University of Washington. Figure 3 shows the validation of the modelling approach for a ductile CBF (equivalent to Type MD CBF in this study) based on a frame tested by [15]. The gusset plate was modelled with the rotational spring suggested by [12]. No rotational limit was implemented as discussed in Sect. 3.1, assuming that the demand critical weld and adequate clearance for out-of-plane rotation is provided. The brace fracture was modelled by the MSR material proposed by [24]. In the case of Type CC, the overall approach was the same, except with the addition of gusset plate interface weld fracture. Figure 4 shows the validation of this model based on a frame tested by [4]. The sudden drop of strength is attributed to the gusset plate interface weld fracture, which was modelled as discussed in Sect. 3.1. Two other modes of damage, namely brace-to-gusset weld fracture and axial yielding of the gusset plate, were also considered during the validation against the test result from [4]. However, for the sake of simplicity, these two modes were omitted while modelling the prototype buildings for the current study because, during the validation, failure occurred due to the gusset plate interface weld and brace fracture at a much earlier stage than developing the capacity of the brace-to-gusset weld and axial yielding of the gusset plate, indicating that the two omitted damage modes were not as dominant compared to the modelled ones.

4 Ground Motion Selection and Scaling

A suite of 22 ground motions, each having two horizontal components, was selected and scaled according to FEMA P695 (2009). This ground motion record set was then collectively scaled at various increments, from one-third to two times the DGM (2%

Fig. 3 Validation of the numerical model for type MD (experimental results from [15])

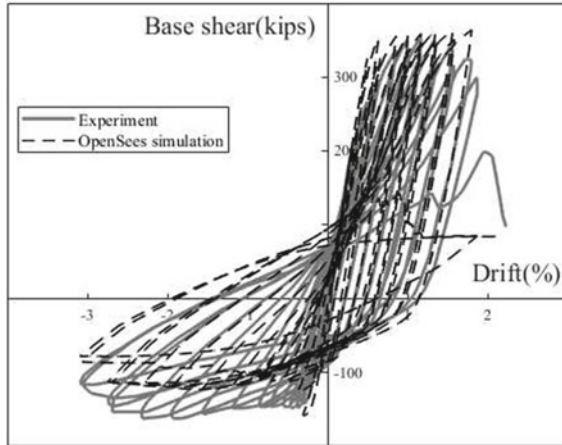
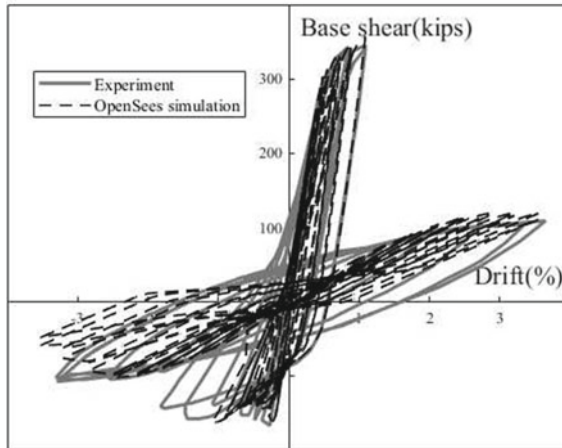


Fig. 4 Validation of the numerical model for type CC (experimental results from [4])



probability of being exceeded in 50 years, as per the [20]). The scaled spectra of all records, the corresponding median spectrum, and the target spectrum are shown in Fig. 5. Figure 5 also shows the spectrum for the Imperial Valley ground motion, which is used in Sect. 5.1. The median of the scaled spectra matches the target spectrum at the fundamental period of the structure but underestimates the target at longer periods.

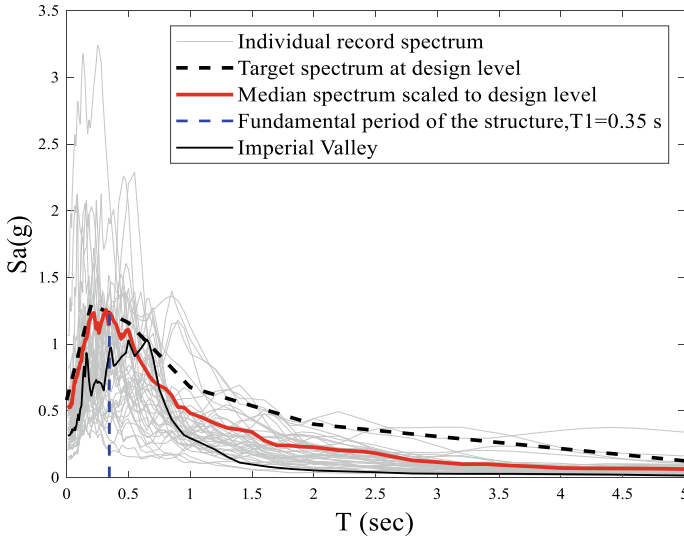


Fig. 5 Scaling according to FEMA P-695

5 Results and Discussion

5.1 Response to a Single Ground Motion

Figure 6 shows the inter-storey drift ratio (IDR) of the three floors of the Type MD CBF, subjected to the single record (Imperial Valley) at the DGM level. As discussed earlier, brace fracture was the only failure mode in the Type MD CBF. In both Types MD and CC, the onset of the brace fracture was captured by monitoring the stress–strain behaviour of the extreme fibre of the brace element, and hence, the “brace fracture” does not mean the complete fracture of the brace but rather the onset of fracture at the extreme fibre. Sequential occurrence of the different damage states for Type MD is shown Fig. 6. In the current study, several damage states were considered: (i) buckling or yielding of the braces (grouped as DS1), (ii) the onset of the brace fracture and gusset plate fracture (grouped as DS2); and (iii) probable collapse (DS3), where the maximum inter-storey drift exceeds 5% [11]. None of the six braces initiated fracture during the earthquake, and the storey drift was reasonably similar at all levels but slightly larger at the second storey, which is consistent with the average results discussed in Sect. 5.2.

Figure 7 shows the storey drift history for the Type CC CBF, subjected to the same ground motion with the same scaling. For this frame, the right brace buckled first, followed by the left brace. After a few seconds, the right brace fractured, causing an excessive rotational demand at the gusset plate that immediately led to fracture of the gusset plate interface weld, and thus the whole brace module lost its strength. A much higher value of IDR is observed in the top storey compared to the bottom

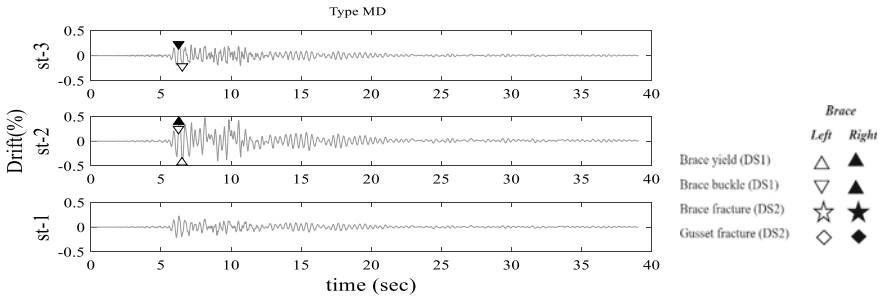


Fig. 6 Inter-storey drift ratio for three stories, showing the sequential damage states for type MD during Imperial Valley

storeys. Figure 8 demonstrates the force–deformation hysteresis of the right brace of the top storey. Any further brace fracture or gusset plate interface weld fracture was not observed in the left brace, while the middle of the third-floor beam deflected severely (more than 150 mm) both upward and downward. This severe deflection at the middle of the beam prevented the left brace from developing forces that would lead to any further damage mode. For comparison, in the case of the Type MD CBF, the deflection of the third-floor beam was limited to 2.5 mm and only in downward direction.

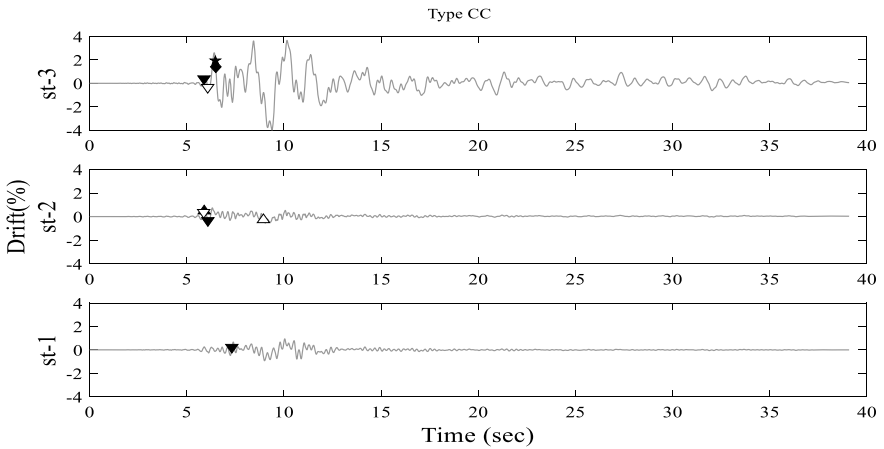
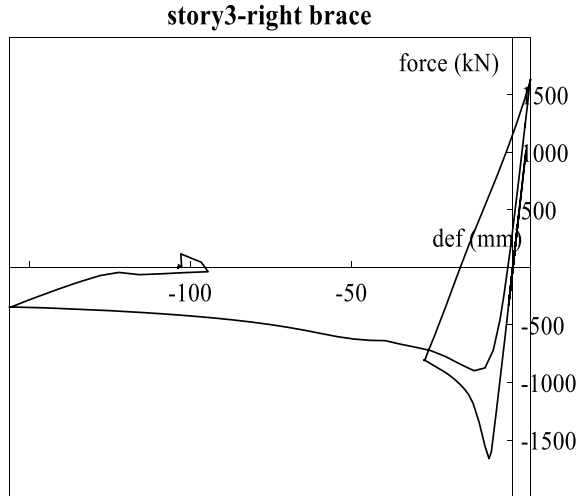


Fig. 7 Damage states shown on the inter-storey drift ratios for the type CC during the Imperial Valley ground motion

Fig. 8 Force deformation hysteretic behaviour of the third storey right brace



5.2 Response to the Suite of Ground Motions at DGM Level

Figure 9 shows the mean and mean + standard deviation of the IDR for both frame types at the DGM level earthquake. In case of the Type MD design, the mean IDR of each storey is within a similar range and much lower compared to that of the Type CC design. In the case of Type CC design, the IDR at the top storey level is generally much higher than at the bottom two storeys. Also, the top storey shows a much higher dispersion relative to the mean IDR. The Type CC CBF was designed for a much higher base shear than the Type MD CBF, with the braces intended to be nearly elastic. However, the beams in the Type CC CBF were not capacity protected for the unbalanced vertical force after brace buckling, and the top beam was most vulnerable in this regard, having no bracing above to mitigate the effect of the chevron bracing in the third storey. As was seen for one typical case in Sect. 5.1, after fracturing one of the braces in the third storey, the third-floor beam often yielded and deformed vertically, preventing the remaining brace from exhibiting its intended nonlinear response and resulting in a very high IDR at the top storey (Fig. 9).

In case of the Type CC CBF, DS2 comprises two different modes of failure: (i) when the brace started fracturing prior to the gusset plate and (ii) when gusset fracture happened first. There was no case where the brace started fracturing but did not eventually lead to a gusset plate interface weld fracture. Conversely, in some cases the gusset plate interface weld fractured first, which immediately detached the brace module from the frame and did not allow the brace fracture to take place. The distribution of these two modes of failure is described in Table 3. While the contribution of “gusset fractured first” is less compared to “brace fracture started first,” it is not negligible.

Fig. 9 Average trend of the storey drift ratio in type MD and CC

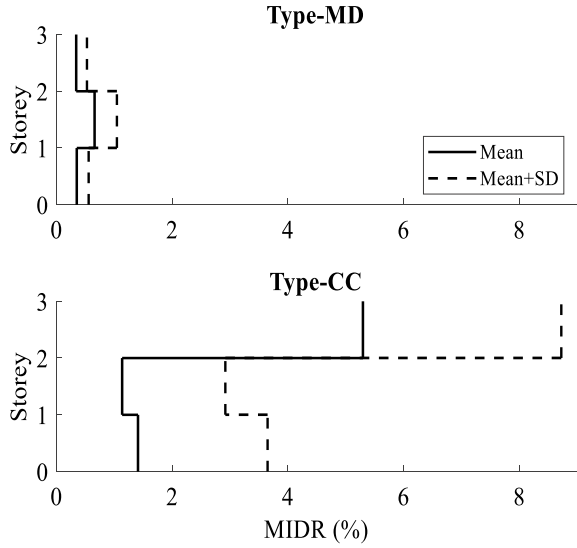


Table 3 Distribution of two types of fracture mechanics in DS2 of Type CC; all entries represent the number of occurrences out of 44 EQs

| IM | Storey | Brace fracture started first | Gusset fractured first |
|---------|--------|------------------------------|------------------------|
| 0.33DGM | 1 | 0 | 0 |
| | 2 | 0 | 0 |
| | 3 | 4 | 2 |
| 0.67DGM | 1 | 0 | 1 |
| | 2 | 1 | 0 |
| | 3 | 24 | 8 |
| DGM | 1 | 2 | 8 |
| | 2 | 5 | 1 |
| | 3 | 28 | 8 |
| 1.5DGM | 1 | 16 | 13 |
| | 2 | 20 | 1 |
| | 3 | 32 | 7 |
| 2.0DGM | 1 | 34 | 8 |
| | 2 | 28 | 0 |
| | 3 | 34 | 9 |

5.3 Multiple Stripe Analysis

Multiple stripe analysis (MSA) was conducted, where dynamic analysis was performed with the suite of 44 ground motions at a variety of intensity measure

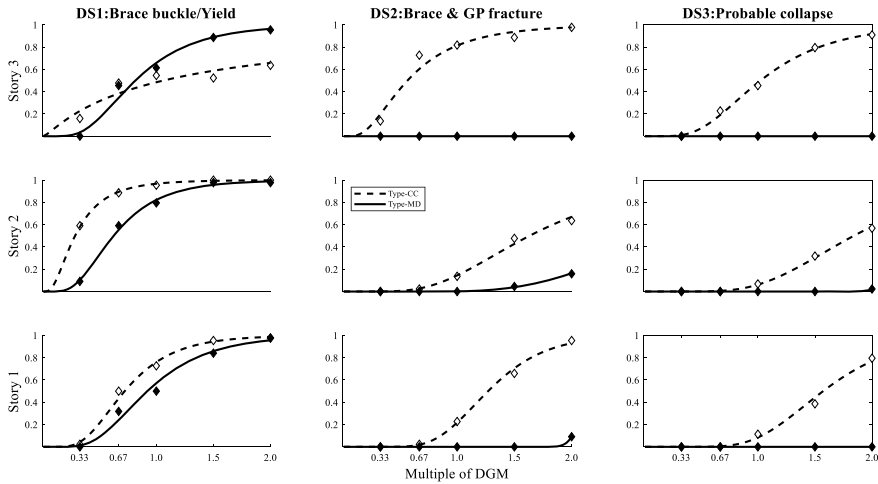


Fig. 10 Fragility curve drawn over the separate storey level, for three different damage states considered

(IM) levels and the number of occurrences or exceedances of any damage state was noted at each IM level. In the current study, five IM levels were considered: 0.33, 0.67, 1.0, 1.5, and 2.0 times the DGM. Considering the three damage states discussed earlier, the fragility curves were fitted using a lognormal distribution based on the maximum likelihood estimation method [3]. Figure 10 shows the fragility curves drawn over the three storey levels to understand the behaviour of the system, such as drift accumulation or the variation in the number of different fracture mechanisms over the storey levels.

Figure 10 demonstrates that the probability of reaching DS1 (brace buckles or yields) is similar for both designs at the first storey, whereas Type CC CBF shows higher probability of failure than the Type MD CBF at the second storey. A well-designed Type MD shows a similar fragility curve at all storeys, whereas the Type CC design shows a lower probability of reaching DS1 than the Type MD design at the top storey for intensities at and above the DGM, but higher probabilities of reaching DS1 at other storeys and intensities. In the case of the Type MD design, the probability of exceeding DS2 and DS3 is zero for almost all cases. Conversely, the probability of the Type CC CBF reaching or exceeding DS2 or DS3 in at least one level is 50% or higher for all intensities at or above the DGM. Overall, at DS1, the performance of the two design types is comparable, but a significant difference in failure probability is noticed at DS2 and DS3.

6 Conclusion

A pair of CBF systems was designed based on the provisions for Type MD and Type CC in CSA S16:19. The CBFs were modelled numerically in OpenSees to capture both brace fracture and gusset plate interface weld fracture, and the seismic performance was compared. First, the sequential occurrence of damage states observed during NLRHA of a typical record at the DGM level was discussed. The IDRs at different storey levels of the Type MD CBF were generally similar, whereas for the Type CC design, the IDR was much higher at the third storey because of the yielding and deflection of the top floor beam due to the unbalanced vertical force demand after brace buckling. Overall, the mean and dispersion of IDR were much higher for the Type CC design than for the Type MD design, especially at the top storey. Considering three levels of damage states, storeywise fragility curves were drawn. At DS1, the performance of the two types of design was comparable. However, the probability of exceeding DS2 and DS3 was much higher for the Type CC CBF than for the Type MD CBF. This suggests that, while both designs equally satisfied the building code requirements, the risk of both seismic loss and collapse with the Type CC design was significantly higher than for the Type MD design. Further study is needed to determine whether this result is true more generally for other buildings and types of connections, as well as how various design parameters affect the seismic fragility of the structure.

Acknowledgements The authors gratefully acknowledge the support of this study from Discovery Grant funding provided by the Natural Sciences and Engineering Research Council (NSERC) of Canada. Any opinions, findings, and conclusions or recommendations expressed in this material are those of the authors and do not necessarily reflect the views of the sponsors.

References

1. ANSI/AISC 341-16 (2016) Seismic provisions for structural steel buildings. American Institute of Steel Construction, Chicago, Illinois
2. ASCE/SEI 7-22 (2022) Minimum design loads and associated criteria for buildings and other structures. American Society of Civil Engineers
3. Baker JW (2015) Efficient analytical fragility function fitting using dynamic structural analysis. *Earthq Spectra* 31(1):579–599
4. Ballard R (2015) Impact of connection type on performance of non-seismic concentrically braced frames. Thesis submitted in partial fulfillment of the requirements of Master of Science, Dept. of Civil Engineering, University of Washington
5. Bradley CR, Fahnestock LA, Hines EM, Sizemore JG (2017) Full-scale cyclic testing of low-ductility concentrically braced frames. *J Struct Eng* 143(6):04017029
6. Castonguay PX (2009) Seismic performance of concentrically braced steel frame of the conventional construction category. Thesis submitted in partial fulfillment of the requirements of a Master's degree in applied sciences, Dept. of Civil Engineering, Ecole Polytechnique De Montreal
7. CSA S16:19 (2019) Design of steel structures. Canadian Standards Association, Toronto, Ont., Canada

8. Elkady A, Lignos DG (2015) Effect of gravity framing on the overstrength and collapse capacity of the steel frame building with perimeter special moment frames. *Earthquake Eng Struct Dynam* 44:1289–1307
9. FEMA P-695 (2009) Quantification of building seismic performance factors. Prepared by Applied Technology Council. Prepared for Federal Emergency Management Agency
10. Herman D (2007) Further improvements on and understanding of special concentrically braced frame systems. Thesis submitted in partial fulfillment of the requirements of Master of Science, Dept. of Civil Engineering, University of Washington
11. Hsiao PC, Lehman DE, Berman JW, Roeder CW, Powell J (2014) Seismic vulnerability of older braced frames. *J Perform Constr Facil* 28(1):108–120
12. Hsiao PC, Lehman DE, Roeder CW (2012) Improved analytical model for special concentrically braced frames. *J Constr Steel Res* 73:80–94
13. Hsiao PC, Lehman DE, Roeder CW (2013) A model to simulate special concentrically braced frames beyond brace fracture. *Earthquake Eng Struct Dynam* 42:1–6
14. Johnson MM (2014) Seismic evaluation of bolted connections in non-seismic concentrically braced frames. Thesis submitted in partial fulfillment of the requirements of Master of Science, Dept. of Civil Engineering, University of Washington
15. Johnson SM (2005) Improved seismic performance of special concentrically braced frames. Thesis submitted in partial fulfillment of the requirements of Master of Science, Dept. of Civil Engineering, University of Washington
16. Kotulka BA (2007) Analysis for a design guide on gusset plates used in special concentrically braced frames. Thesis submitted in partial fulfillment of the requirements of Master of Science, Dept. of Civil Engineering, University of Washington
17. Lehman DE, Roeder CW, Herman D, Johnson S, Kotulka B (2008) Improved seismic performance of gusset plate connections. *J Struct Eng* 134(6):890–901
18. Liu J, Astaneh-Asl A (2004) Moment-rotational parameters for composite shear tab connections. *J Struct Eng* 130(9):1371–1380
19. McKenna FT (1997) Object-oriented finite element programming framework for analysis, algorithm and parallel computing. Ph.D. thesis, Dept. of Civil Engineering, University of California, Berkeley
20. NBC (2015) National building code of Canada. National Research Council of Canada. Canadian Commission on Building and Fire Codes
21. Powell JA (2009) Evaluation of special concentrically braced frames for improved seismic performance and constructability. Thesis submitted in partial fulfillment of the requirements of Master of Science, Dept. of Civil Engineering, University of Washington
22. Roeder CW, Lumpkin EJ, Lehman DE (2011) A balanced design procedure for special concentrically braced frame connections. *J Constr Steel Res* 67(11):1760–1772
23. Rudman A, Tremblay R, Rogers CA (2021) Conventional I-shape brace member bolted connections under seismic loading: laboratory study. *J Constr Steel Res* 184
24. Sen AD, Roeder CW, Lehman DE, Berman JW (2019) Nonlinear modeling of concentrically braced frames. *J Constr Steel Res* 157:103–120
25. Sen AD, Sloat D, Ballard R, Johnson MM, Roeder CW, Lehman DE, Berman JW (2016) Experimental evaluation of the seismic vulnerability of braces and connections in older concentrically braced frames. *J Struct Eng* 142(9):04016052
26. Sizemore JG, Fahnestock LA, Hines EM, Bradley CR (2017) Parametric study of low-ductility concentrically braced frames under cyclic static loading. *J Struct Eng* 143(6):04017032
27. Sloat D (2014) Evaluation and retrofit of non-capacity designed braced frames. Thesis submitted in partial fulfillment of the requirements of Master of Science, Dept. of Civil Engineering, University of Washington
28. Swatosh MA (2016) Seismic evaluation and retrofit of concentrically braced frames. Thesis submitted in partial fulfillment of the requirements of Master of Science, Dept. of Civil Engineering, University of Washington
29. Wang C, Tremblay R, Rogers CA (2021) Component-based model for bolted brace connections in conventional concentrically braced frames. *Eng Struct* 247